9-Aryl-3-aminocarbazole as an Environment- and Stimuli-Sensitive Fluorogen and Applications in Lipid Droplet Imaging

Matsubara, Ryosuke ; Kaiba, Tomoaki ; Nakata, Akito ; Yabuta, Tatsushi ; Hayashi, Masahiko ; Tsubaki, Motonari ; Uchino, Takashi ; Chatani,…

(Citation)
Journal of Organic Chemistry,84(9):5535-5547

(Issue Date)
2019-05-03

(Resource Type)
journal article

(Version)
Accepted Manuscript

9-Aryl-3-aminocarbazole as an environment- and stimuli-sensitive fluorogen and applications in lipid droplet imaging

Ryosuke Matsubara,* Tomoaki Kaiba, Akito Nakata, Tatsushi Yabuta, Masahiko Hayashi, Motonoari Tsubaki, Takashi Uchino, Eri Chatani

Department of Chemistry, Graduate School of Science, Kobe University, Nada, Kobe 657-8501, Japan

ABSTRACT: Environment-sensitive luminophoric molecules have played an important role in the fields of smart materials, sensing, and bioimaging. In this study, it was demonstrated that depending on the substituents, 9-aryl-3-aminocarbazoles can display aggregation-induced emission and solvatofluorochromism, and the operating mechanism was clarified. The application of these compounds to lipid droplet imaging and fluorescent probes for cysteamine was demonstrated.

INTRODUCTION

Environment-sensitive luminophoric properties have attracted attention owing to their potential applicability to smart materials, sensing, and bioimaging.[1-5] Aggregation is an environmental factor regulating the luminescent property. Numerous luminophoric compounds generally exhibit aggregation-caused quenching (ACQ) and emit reduced fluorescence upon aggregation, which is ordinarily caused by intermolecular π–π stacking interaction to quench the excited luminophore.[6-7] In contrast, certain luminogenic molecules enhance the emission upon aggregation; this phenomenon is called aggregation-induced emission (AIE).[8-9] Extensive research has been performed since the development of the AIE concept.[10] Hexaphenylsilole and tetraphenylethene are the prototypical molecules with AIE property,[11] and numerous other types of structural motifs have also emerged as AIE luminophores.[12-13] Solvent polarity is another environmental factor that dramatically influences the fluorescent attributes such as color and intensity.[14-19]

A majority of the molecules exhibiting AIE and/or a solvatofluorochromic nature contain plural aromatic moieties connected with each other via several single bonds, composing an overall large π-conjugated system. Herein, we report that a relatively small unit, 9-aryl-3-aminocarbazole (the minimum required unit size is ~300 Da), endows the molecules with both AIE and solvatofluorochromic properties. The presence of an amino group at the three-position of the carbazole and of an electron-deficient aromatic substituent at the nine-position was the prerequisites for the AIE property. The operating mechanism of the observed AIE phenomenon is discussed. The application of solvatofluorochromism was demonstrated through light up detection of lipid droplets (LDs) in living cells with low background noise.

RESULTS

Synthesis

A series of *N*-arylcarbazoles (NACs) were synthesized as shown in Figure 1. We set 3,6-bis(dimethylamino)carbazole (**14**) as a key common intermediate, with which various bis(dimethylamino)carbazole derivatives were synthesized.[20] Shortly after the investigation was started, we realized that the synthesis of **14** was not trivial. The initial attempt to directly synthesize **14** from 3,6-dibromocarbazole (**9**) yielded a moderate quantity, albeit as a mixture with byproducts derived from the bond-forming reaction with carbazole nitrogen. The separation of **14** from the other byproducts was exceptionally challenging. Moreover, this reaction exhibited low reproducibility depending on the reaction scale; this can be attributed to the volatility of dimethyl amine at the applied reaction temperature. Therefore, we adopted the protective group strategy to overcome this issue. The NH group of **9** was protected with benzyl-type protective groups to yield carbazole **10** and **11**. The subsequent introduction of NMe_2 groups proceeded well; reasonable yields of bis(dimethylamino)carbazoles **12** and **13** were obtained. The removal of the *N*-benzyl-type protection was initially attempted by hydrogenation using transition metal catalysts such as Pd/C, $Pd(OH)_2$/C, Raney Ni, and Wilkinson's catalyst with or without pressurizing hydrogen gas. All trials failed with the starting material completely recovered; this was likely to be a result of the considerable electron-richness of carbazole moiety. The DDQ-oxidation for *p*-methoxybenzyl-protected carbazole **13** was unsuccessful owing to the lability of electron-rich carbazole toward oxidation. Meanwhile, the treatment of **13** with BCl_3 provided a reasonable yield of **14**. On the other hand, mono-NMe_2 carbazole **16** could be synthesized without protective group manipulation. The mono-bromination of parent carbazole using an equivalent of *N*-bromosuccinimide (NBS) followed by palladium-catalyzed amination provided a good yield of **16**. The *N*-arylation of **14** and **16** was achieved by copper-catalyzed coupling reaction, yielding NAC **1**–**5**. NAC **6** and **7** were synthesized by the copper-catalyzed *N*-arylation of the corresponding known N–H carbazoles. The synthesis of julolidine-type NAC **8** was accomplished by nitration of NAC **6** followed by reduction, *N*-alkylation, and cyclization.

Photophysical properties

The photophysical properties of NACs **1**–**8** were analyzed by UV-Vis and emission spectroscopies. The absorption and emission maximum as well as the photoluminescence (PL) quantum yields in solution state (Φ_s) are presented in Table 1. The PL quantum yields in solid state (Φ_s) for the selected NACs are also presented. The data, except those for Φ_s, were obtained

from deoxygenated THF solution. The solid-state quantum yields were measured for the powder materials obtained after grinding the microcrystals obtained initially.

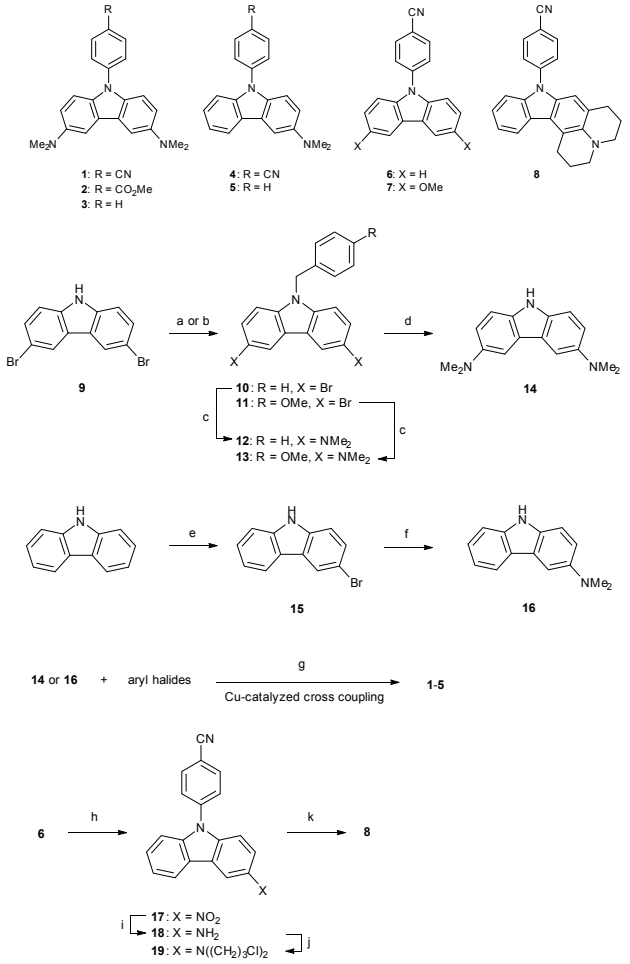

Figure 1. Synthesis of NAC **1**–**8**. Conditions: a) BnBr (2.0 equiv), K_2CO_3 (10 equiv), DMF, room temperature (rt), 71%. b) NaH (1.5 equiv), *p*-(MeO)$C_6H_4CH_2Cl$ (1.5 equiv), DMF, rt, 99%. c) $Pd_2(dba)_3$ (1 mol%), Ruphos (2.4 mol%), LiHMDS (6.0 equiv), Me_2NH_2Cl (3.0 equiv), tetrahydrofuran (THF), 80 °C, 83% (**12**), 97% (**13**). d) BCl_3 (6.0 equiv), CH_2Cl_2, rt, then 4 M HCl aq., 86%. e) NBS (1.0 equiv), THF, rt, 89%. f) $Pd_2(dba)_3$ (1 mol%), Ruphos (2.4 mol%), LiHMDS (6.0 equiv), Me_2NH_2Cl (3.0 equiv), THF, 80 °C, 73%. g) For **1**, **2**, and **4**; ArI (1.1 equiv), LiCl (1.0 equiv), CuI (10 mol%), 1,10-phenanthroline (10 mol%), Cs_2CO_3 (1.2–1.3 equiv), DMF, 150 °C, 65% (**1**), 64% (**2**), 67% (**4**). For **3** and **5**; PhBr (10 equiv), CuI (1.1 equiv), K_2CO_3 (3.9 equiv), $AcNMe_2$, 180 °C, 76% (**3**), 80% (**5**). h) HNO_3 (17 equiv), AcOH, 72%. i) Pd/C (10 mol%), H_2 (1 atm), MeOH, rt, 33%. j) 1-Br-3-Cl-pentane (15 equiv), Na_2CO_3 (4.0 equiv), 100 °C. k) DMF, 160 °C, 26% (2 step).

AIE properties were evident in NACs **1**, **2**, and **4**, which have electron deficient aryl substituents at the nine-position and NMe_2 group at the three-position of the carbazole unit; their quantum yields in THF solution were low (Φ_f were 1.6%, ~0%, and 1.5%, respectively), whereas they were emissive in the solid state (Φ_s were 15%, 4.4%, and 20%, respectively). The PL difference between the solution and solid states of NAC **1** is visually observable (Figure 2). In contrast, NACs **3** and **5** with an electronically neutral arene (phenyl group) at the nine-position of the carbazole unit exhibited strong emission in THF solution (Φ_f are 35% and 96%, respectively); this indicated that an electron deficient aryl substituent at the nine-position is required for manifesting AIE property. The NMe_2 group at the three-position is also necessary to quench the fluorescence in the solution state: NACs **6** and **7** with electron deficient aryl group at the nine-position albeit without the NMe_2 group at the three-position, are strongly fluorescent in THF (Φ_f are 34% and 31%, respectively). For NAC **8** (similar in structure to NAC **4** except for a non-rotatable C–N single bond at the three-position owing to the julolidine polycyclic structure), the PL quantum yield in THF solution was low (Φ_f = ~0%).

Table 1. Optical properties of NAC luminophores 1–8[a]

NAC	λ_{ab} (nm)	λ_{em} (nm)[b]	Φ_f (%)	Φ_s (%)
1	337, 384	578	1.6	15
2	337, 379	n.d.	~0	4.4
3	327, 389	430	35	–[c]
4	358	570	1.5	20
5	374	425	96	–[c]
6	326, 336	395	34	5.1
7	351, 365	459	31	14
8	374	n.d.	~0	–[c]

[a] λ_{ab} = absorption maximum, λ_{em} = emission maximum, Φ_f = fluorescence quantum yield in solution (solvent: THF), Φ_s = solid state (powder) fluorescence quantum yield. [b] Measured by exciting at the absorption maxima. n.d. = Signal is very weak and not detectable. [c] Amorphous.

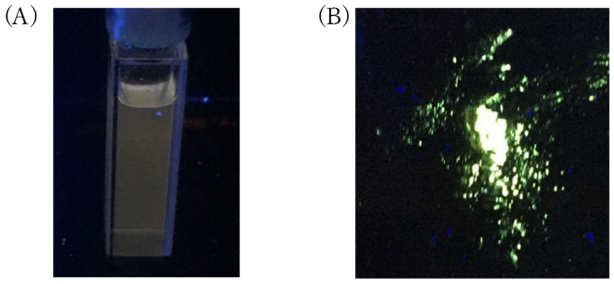

Figure 2. Representation of AIE nature of NAC **1**. Photographs of (A) 10-μM THF solution and (B) solid state of **1** under UV irradiation (excited by 254 nm and black light irradiation, respectively).

The AIE properties of NAC **1** are further investigated in THF/water mixed solutions with different water fractions (f_w). The emissions from the pure THF solution (f_w = 0%) were weak albeit visible (Figure 3A). However, after the addition of water (yielding an f_w of 10%), the emissions were quenched. The non-emissive behavior continued until the f_w reached 90%. Further addition of water at the f_w of 99% caused the precipitation of NAC **1** in the quartz cell, making the solution slightly opaque. Then, the emissions resumed, although becoming blue-shifted compared to those obtained in pure THF. The fluorescence change was visually observable, as shown in Figure 3B. The dynamic light scattering (DLS) measurement of the solution with an f_w of 99% revealed the formation of particles with dimensions of submicrometer order (Figure 3C), which was

visually evidenced by the Tyndall scattering observed using a laser pointer (Figure 3C, inset) and field emission scanning electron microscopy (FE-SEM) analysis (Figure S7).

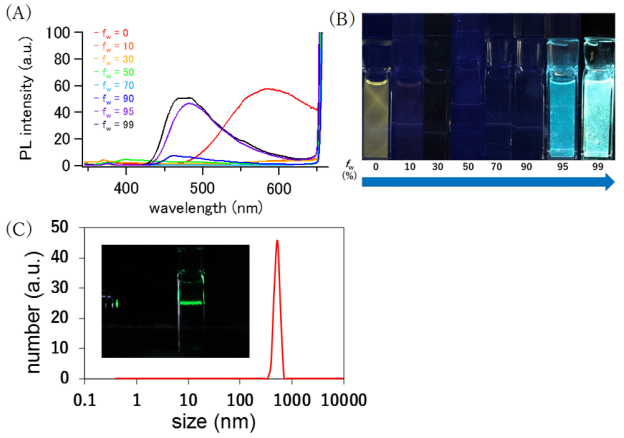

Figure 3. Fluorescence examination of the 10 μM solution of **1** in the THF/water mixed solvents with various water fractions. (A) Luminescence spectra. (B) Photographs under UV irradiation (black light). (C) DLS measurement of the solution of **1** in the THF/water mixed solvent (f_w: 99%). (inset) Tyndall scattering seen using a laser pointer.

Single crystal X-ray diffraction (SCXRD) analysis revealed the molecular structure of the fluorescent solid NAC **1** (Figure 4). A unit cell contained the two independent molecules; one of these is depicted in Figure 4A. The nitrogen atoms of the two dimethyl-amino groups exhibit almost planar geometry (the sum of the three bond angles around the concerned nitrogen is 350.2°); this indicated that the lone pair on the nitrogen of the dimethyl amino groups is conjugated with the π-electrons on the carbazole to a considerable extent. The aryl group on the nine-position nitrogen twisted against the carbazole π-plane with a dihedral angle of 43.1°. With regard to the molecular packing, the molecules are positioned close to each other (Figure 4B): the carbazole and benzonitrile units are placed one above the other with a mutual distance of 3.4Å, indicating the presence of π–π stacking.

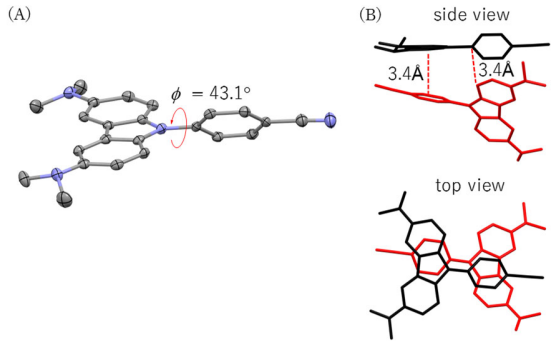

Figure 4. Single-crystal structure of NAC **1**. (A) ORTEP representation of one of the two independent molecules in the unit cell. (B) Packing pattern of molecules.

Because the solid-state fluorescence was measured for the powder materials that were prepared by grinding the microcrystals initially obtained after the recrystallization, the difference between the microcrystals and ground solids was investigated (Figure 5). The microcrystals and powders exhibited similar patterns in the fluorescence spectroscopy and powder X-ray diffraction (PXRD) analysis. These results indicate that the grinding did not change the morphology of the microcrystals significantly, ensuring the validity of basing the discussion of solid fluorescent property on the SCXRD structure.

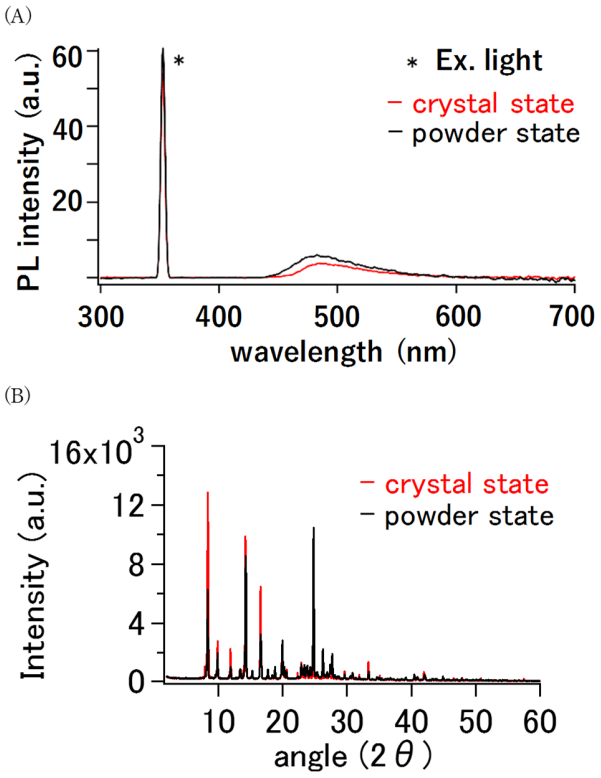

Figure 5. Comparison between the as-prepared microcrystals and ground powder of NAC **1**. (A) Solid PL spectra. (B) PXRD spectra.

The PL properties of NAC **1** as well as of NAC **3** in various solvents are presented in Table 2. The results demonstrate that NAC **1** rather than NAC **3** exhibits solvatofluorochromism nature. The absorption spectra of NAC **1** and **3** exhibited negligible change in solvents with different polarities (which can be quantified by orientation polarizability Δf); this indicated that the ground states of NAC **1** and **3** are negligibly affected by the solvent (Figure S2). However, the fluorescence of NAC **1** was sensitive to the solvent; as the solvent polarity increased, the fluorescence maximum wavelength lengthened (Figure 6A), and the fluorescence quantum yield decreased. The color change of fluorescence could be observed by the naked eyes (Figure 6C). In contrast, the fluorescent property of NAC **3** was insensitive to the solvent polarity (Figure 6BD).

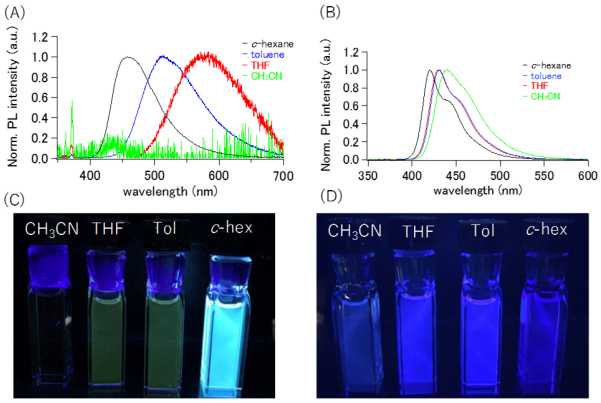

Figure 6. PL properties of NAC **1** and **3** in solution state in various solvents. Solution concentration: 10 μM. Each solution was excited at its absorption maxima. PL spectra of (A) NAC **1** and (B) **3**. Photographs of (C) NAC **1** (λ_{ex} = 365 nm) and (D) **3** (λ_{ex}= 254 nm).

To exhibit the solvent polarity effect on the fluorescence of NAC **1**, we gradually changed the hydrophobicity of the solvent by increasing the hexane fraction (f_h) against THF in the solution of **1**. The non-normalized luminescence spectra demonstrated that as the hydrophobicity increased, the spectrum was blue-shifted, and the intensities of the peaks increased (Figure 7A and B). The luminescence color of **1** changed from yellow to green to blue as the solution hydrophobicity increased (Figure 7C). According to the DLS measurement, the solution of **1** with the f_h of 99% did not contain aggregates (Figure 7D); this indicated that the blue color emission was derived from the isolated form rather than the aggregated state.

Table 2. Solvent effects on PL properties of 1 and 3

		1			**3**		
solvent	Δf^a	λ_{ab} (nm)	λ_{em} (nm)^b	Φ_f (%)	λ_{ab} (nm)	λ_{em} (nm)^b	Φ_f (%)
c-hexane	0	335, 382	458	25	324, 383	420	37
toluene	0.014	339, 387	512	25	329, 390	430	49
THF	0.210	337, 384	578	1.6	327, 389	430	35
CH_3CN	0.306	337, 381	n.d.	~0	323, 387	439	39

[a] Orientation polarizability. [b] Measured by exciting at 335 nm. n.d. = Signal is very weak and undetectable.

To demonstrate the solvent polarity effect on the fluorescence of NAC **1**, we gradually changed the hydrophobicity of the solvent by increasing the hexane fraction (f_h) against THF in the solution of **1**. The non-normalized luminescence spectra demonstrated that as the hydrophobicity increased, the spectrum was blue-shifted, and the intensities of the peaks increased (Figure 7A and B). The luminescence color of **1** was changed from yellow to green to blue as the solution hydrophobicity increased (Figure 7C). According to the DLS measurement (Figure 7D) and atomic force microscopy (AFM) analysis (Figure S8), the solution of **1** with the f_h of 99% did not contain a large size of aggregates; this indicated that the blue color emission was derived from the isolated form rather than the aggregated state.

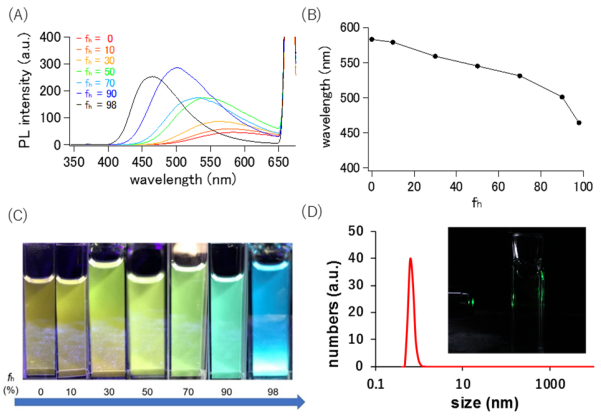

Figure 7. Fluorescence examination for the solution of **1** in THF/hexane mixed solvents with various hexane fractions. (A) Luminescence spectra. (B) Plot of maximum emission wavelength. Solution concentration: 10 μM. λ_{ex} = 400 nm. (C) Photographs under UV irradiation (black light). (D) DLS measurement of the solution of **1** in the THF/hexane mixed solvent (f_h: 98%). Inset figure shows no Tyndall scattering observed (compare with Figure 3C).

Applications

With the knowledge that NAC **1** exhibits polarity-sensitive fluorescence, we investigated its capability to stain LDs in living cells (Figure 8). For comparison, Nile Red,[21] a commercially available fluorescent stain for LDs, was used in parallel with NAC **1**. The living HeLa cells were pre-incubated with oleic acid to form LDs.[22] Then, Nile Red and NAC **1** were incubated in independent batches of cultured cells, followed by washing with PBS buffer. The fluorescence from each batch was analyzed by a confocal fluorescence microscope. The LDs were lit up by using Nile Red (Figure 8A and C). However, the whole cytoplasm was vaguely stained, resulting in the low S/N ratio, as indicated previously.[23] NAC **1** was cell membrane permeable and absorbed in the cell. Moreover, NAC **1** selectively lit up the LDs with low background fluorescence (Figure 8B and D); this is likely to be because of the strong dependence of the fluorescence intensity of NAC **1** on the surrounding polarity (Figure 3 and Figure 6). No noticeable cytotoxicity of **1** was observed at the tested concentration (12 μM) and further cytotoxicity investigation with higher concentration was hampered owing to the poor solubility of **1**.

To further explore the application of the unique photophysical properties of the developed NAC, we designed a stimuli-sensitive turn-on fluorescent molecule based on the

NAC architecture. Considering that an electron deficient substituent on the phenyl group at the nine-position is required for the emission quenching of the solution in a polar solvent, we synthesized NAC **20** with an electrophilic formyl group on the phenyl group (Figure 9). The formyl group is adequately electron-withdrawing to ensure the emission quenching of **20** in the solution state in CH_3CN. Upon the addition of cysteamine, NAC **20** was smoothly converted to fluorescent 1,3-thiazolidine **21**; thus, NAC **20** functioned as a turn-on fluorescent probe for cysteamine.

DISCUSSION

Environment-sensitive luminophoric molecular units can operate, by themselves or by being incorporated into the molecules of interest, as a switching module for the fabrication of the molecular sensing probes. Because they are generally used in biological systems, the minimum structural motif required for the manifestation of the switching function should be minimized to secure cell permeability and to minimize the interference in the original function of the parent molecule. This report illustrates a simple 3-aminocarbazole with an electron deficient aryl group at the nine-position to obtain AIE and solvatofluorochromic capabilities.

As shown in Figure 1, their synthesis is straightforward, short-step, and modular; here, *N*-H carbazole **14** or **16** can be used as a common intermediate for a variety of NACs with potential environment-sensitive fluorescence property.

NAC **1**, **2**, and **4** exhibit a low intensity of fluorescence in THF solution and are bright in the solid state (Table 1); i.e., they are AIE molecules.[8] Carbazole is an intrinsically luminogenic molecular unit and is wide applied in organic light emitting diodes (OLED) and chemical probes;[24] this is consistent with the fluorescence emission of NAC **1**, **2**, and **4** in the solid state. However, their indistinct fluorescence in the solution state is uncommon.[25-27] Strong fluorescence was observed from their variant NAC **3** and **5**–**7**, where an electron withdrawing substituent on the nine-position aryl group or an amino group on the carbazole is omitted (Table 1). These results indicate that a combination of strongly electron-rich carbazole and electron deficient aryl group results in the quenching of the potential fluorescence of carbazole in the solution state.

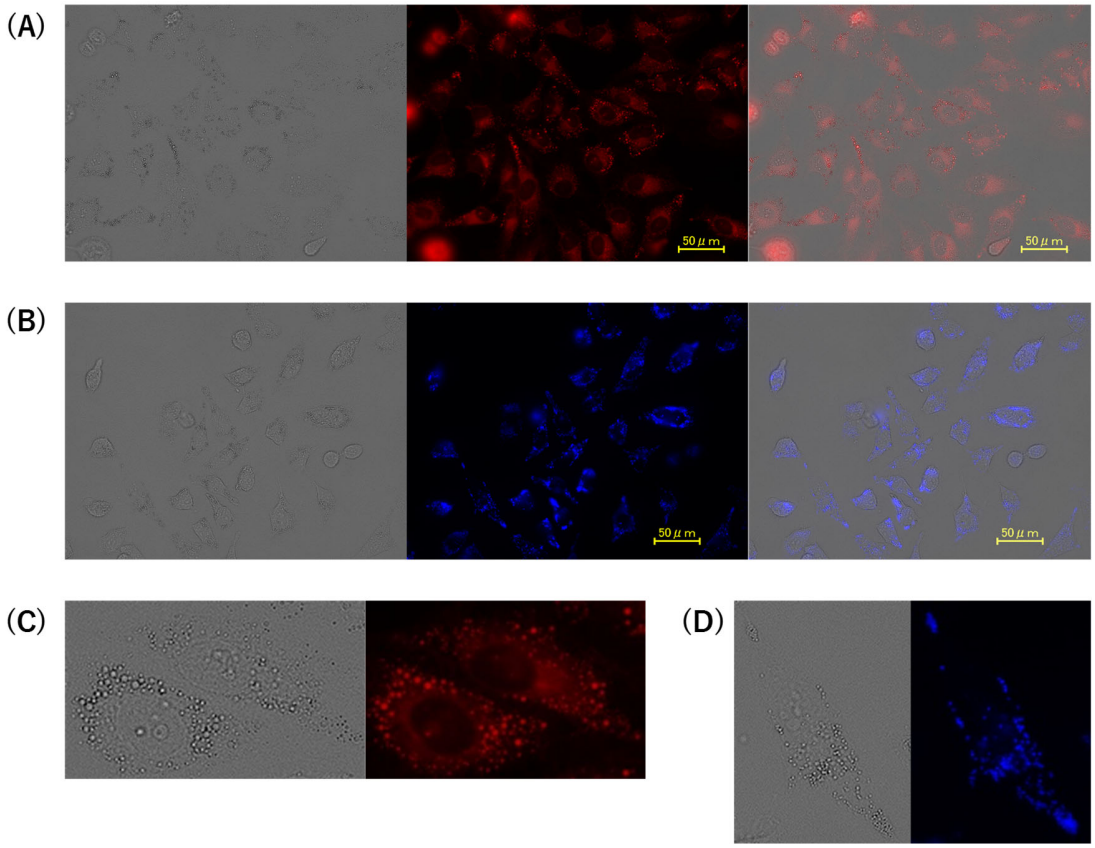

Figure 8. Confocal fluorescence images of living HeLa cells pre-incubated with 62.5-μM oleic acid. (A) and (B) After incubation with Nile Red (30 μM) (A) and NAC **1** (12 μM) (B). Left, bright-field image; middle, fluorescence image; right, merged image. (C) and (D) Magnified images of (A) and (B), respectively. Left, bright-field image; right, fluorescence image. Red staining was produced by exciting at 545 ± 13 nm with the emission filter set at 605 ± 35 nm. Blue staining was produced by exciting at 360 ± 20 nm with the emission filter set at 460 ± 25 nm.

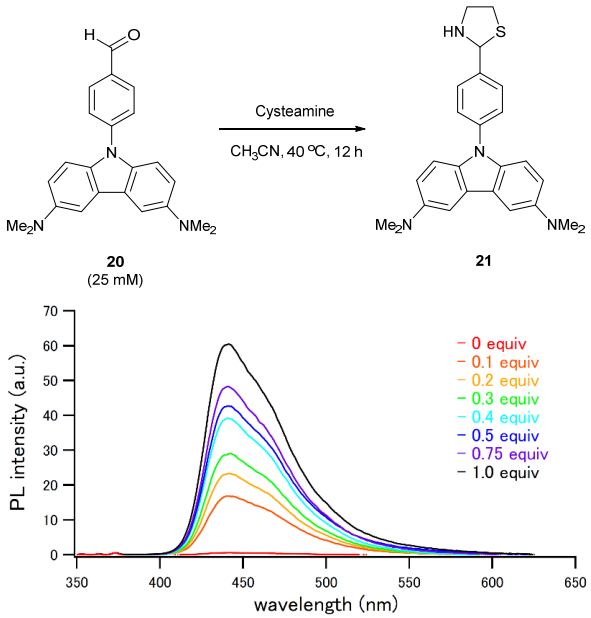

Figure 9. Fluorescence change of **20** upon treatment with cysteamine. λ_{ex} = 335 nm.

It is established that molecules having an electron donor (D) and an electron acceptor (A) tend to generate the intramolecular charge transfer (ICT) excited state. NAC **1**, **2**, and **4** belong to this category. The ground states of NAC **1**, **3**, and **6** were theoretically simulated using DFT at the B3LYP level of theory employing the 6-31G(d,p) basis set in THF (Figure 10). With regard to NAC **1** and **6**, the HOMO is located on the carbazole part and the LUMO on the nine-position aryl group. In contrast, both the HOMO and LUMO of NAC **3** are distributed on the carbazole part. Therefore, it is likely that the transition from HOMO to LUMO upon photoirradiation would result in the ICT excited state for NAC **1** and **6**, and locally excited (LE) state for NAC **3**.

Because of the charge-separated nature, the ICT excited state exhibits a large dipole moment and is stabilized by polar solvents. Therefore, the more polar the solvent is, the smaller the energy gap between S_0 and S_1 is, and the more red-shifted the fluorescence becomes (Figure 7 and Table 2). According to the energy gap law,[28] a smaller Φ_f in polar solvents is reasonable; however, the observed Φ_f of NAC **1** in the polar solvents is still excessively marginal (e.g., Φ_f is approximately zero in acetonitrile, Table 2).

This magnified luminescence-quenching phenomenon can be explained by considering a twisted intramolecular charge transfer (TICT) excited state.[29-31] NAC **1** would acquire the ICT excited states with the π-planes of the D and A units being more twisted via the single bond rotation (bond a in Figure 11C) than it is in the ground state. In this TICT excited state, the orbitals on the D and A units are less conjugated, resulting in the enhanced charge separation ($D^{\bullet+}$ and $A^{\bullet-}$); this enable further stabilization of the excited state by polar solvents. The oscillator strength of the transition from S_1 to S_0 is marginal owing to less conjugation of the two SOMOs in the TICT excited state. Moreover, the contribution of the nonradiative pathway, such as the energy loss by the interaction with solvent molecules, becomes dominant owing to the smaller excited energy of the solvent-stabilized S_1 (energy gap law). Overall, NAC **1** in polar solvents becomes almost non-fluorescent. Meanwhile, in the aggregated state, the molecule cannot relax to a further twisted geometry upon photoexcitation; this is owing to the motionally-restricted situation and absence of interaction with solvent molecules (Figure 11B). Accordingly, Φ_s of NAC **1** is significantly higher than Φ_f (Table 1); this implies that NAC **1** is an AIE molecule. The still modest value of Φ_s of NAC **1** is probably owing to the presence of π–π stacking in the packing geometry (Figure 4). The observation of π–π stacking can be easily rationalized by considering that the carbazole is electron rich and the benzonitrile is electron deficient; there should be electrostatic interaction between the carbazole and benzonitrile units.

NAC **6** and **7** can potentially acquire TICT excited states; however, their Φ_f in THF are high (Table 1). The degree to which the twisted geometry contributes to the S_1 state compared to the more planar geometry is determined by the balance between the stabilization effect by the enhanced dipole moment in polar solvents and the destabilization outcome by the charge separation and the loss of mesomeric effect.[29] A hydrogen or MeO group is a weaker electron-donating group than NMe_2; therefore, the radical cation of carbazole unit in the expected TICT excited states of NAC **6** and **7** are not likely to be adequately stabilized. Thus, NAC **6** and **7** acquire the S_1 states with a less twisted geometry and exhibit stronger fluorescence than NAC **1**.

We first surmised the rotation of the single bond between the carbazole and NMe_2 group (bond b in Figure 11C) to be responsible for the TICT excited-state formation.[32-33] To verify this hypothesis, NAC **8** was designed, in which the single bond of concern cannot rotate.[34] As a result, NAC **8** exhibits weak fluorescence in THF similarly as NAC **1** or **4** (Table 1); this indicates that contrary to our initial conjecture, the TICT excited state is formed via twisting between the carbazole and nine-position aryl group rather than between the carbazole and NMe_2 group (Figure 11C).

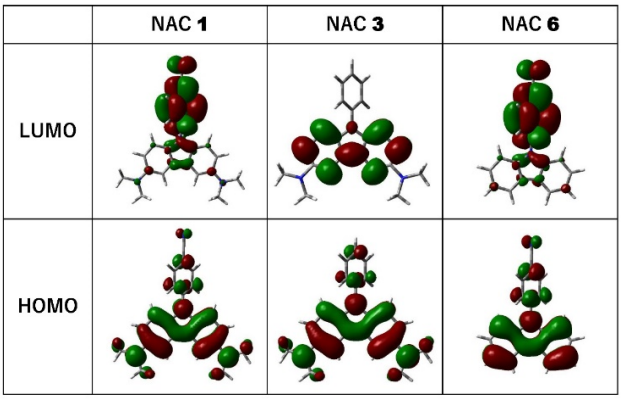

Figure 10. Electron cloud distribution of HOMO and LUMO of NAC **1**, **3**, and **6** calculated using DFT at B3LYP level of theory employing 6-31G(d,p) basis set in THF modeled by PCM approach.

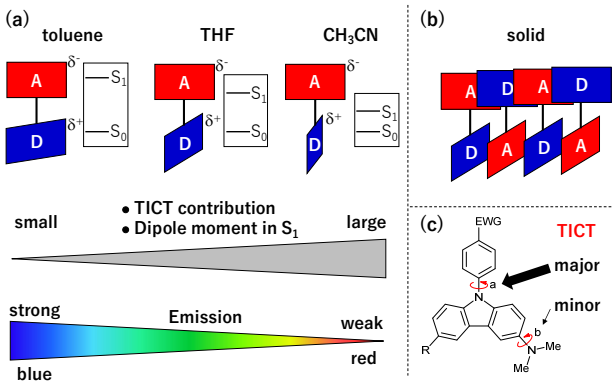

Figure 11. Rationale for environment-sensitive fluorescence property of **1**.

The fluorescence behavior of NAC **1** in the THF/water mixed solvents with various water fractions (Figure 3) can be rationalized as follows:[35-36] In a pure THF solution (f_w = 0%), the fluorescence intensity is weak owing to the TICT excited state; however, they are still visible (Φ_f = 1.5 %). A marginal increase in the solvent polarity (e.g., f_w = 10%) is adequate to completely shut down the fluorescence of NAC **1**. This quenching is persistent until f_w is 90%. A further increase in the water fraction (f_w = 99%) results in the precipitation of NAC **2**; then, the fluorescence derived from the aggregates appears.

LDs are reservoirs of neutral lipids.[37] They are mainly found in adipose tissue but can exist in nearly all cells. Recent studies have shown that LDs not only function as an energy storage but also are involved in other physiological events including membrane formation and maintenance, protein degradation, signal transduction and inflammation.[38] Therefore, the development of selective detection method for LDs is of great importance. Nile Red is a traditional fluorescent probe for LDs but notorious due to a high background noise.[23] Indeed, the low S/N ratio was also observed in our experiments (Figure 8AC). In contrast, NAC **1** is non-emissive in polar environments such as cytoplasm, but becomes fluorescent in lipophilic media such as LD. Expectedly, LDs can be lit up by NAC **1** with a low background noise (Figure 8BD).

Stimuli-sensitive turn-on fluorescent probes can be straightforwardly designed by locating a switchable substituent on the *N*-aryl group, which loses or weakens its electron-withdrawing property upon stimulation. As a proof of concept, NAC **20** with a formyl group on the 9-phenyl ring was designed for detecting cysteamine (Figure 9). The formyl group reacts with cysteamine without a catalyst to form 1,3-thiazoline, which is electronically neutral. As expected, the resulting **21** was emissive in CH_3CN in contrast to **20**, and the increase in the fluorescent intensity of the solution was observed as the amount of adopted cysteamine increased.

CONCLUSION

In this work, we demonstrated 9-aryl-3-aminocarbazole to be an environment- and stimuli-sensitive fluorogen. When the substituent on the 9-aryl group is an electron-withdrawing group such as the cyan and ester groups, the molecules exhibit a highly weak or an absence of fluorescence in polar solvents. This phenomenon could be originating from the TICT excited state, in which the π-planes of the 9-aryl and carbazole units are more twisted than its ground state. In less polar environments, the

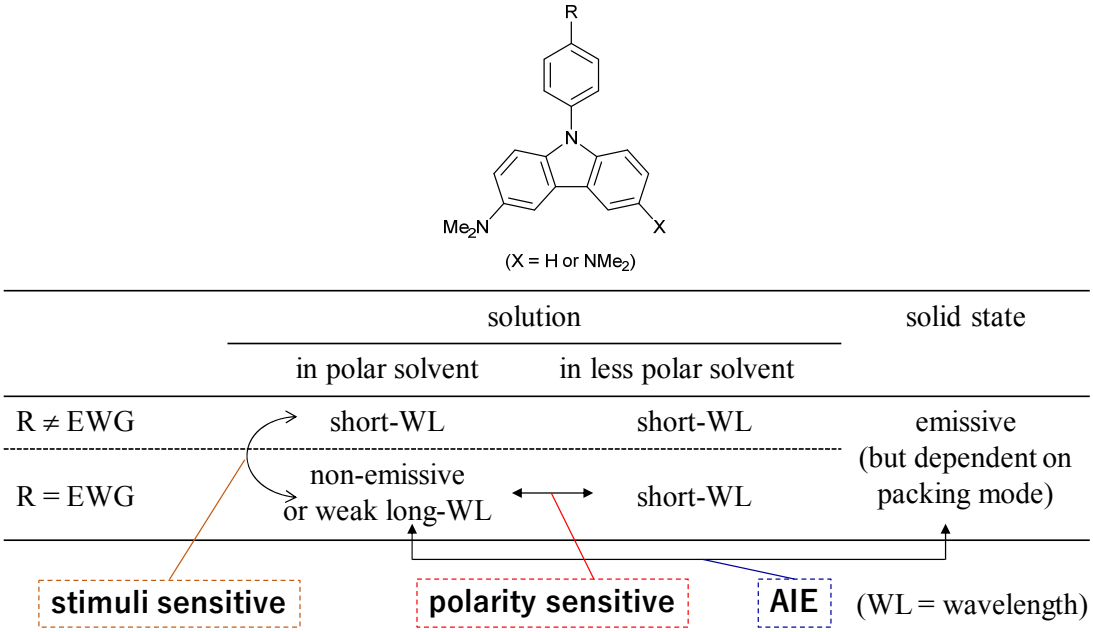

Figure 12. Summary of environment-responsive nature of 9-aryl-3-aminocarbazole

TICT excited state is less dominant in the S_1 state, and the fluorescence intensity increases. Moreover, the fluorescence becomes blue-shifted owing to the raised energy gap of S_0 and S_1; this results from the decrease in the polarity-assisted solvent stabilization of the CT S_1 state. That is, the molecule is endowed with solvatofluorochromism and was therefore applied to LD detection in living cells. The molecule also exhibits AIE property; it becomes emissive in the aggregated form because it cannot generate the TICT excited state. When the substituent on the 9-aryl group is not an electron-withdrawing group, the molecule is emissive regardless of which solvent is used. Exploiting the fluorescence variation depending on the 9-aryl

substituents, we designed the turn-on fluorescent probe for cysteamine detection. The fluorescent behavior of 9-aryl-3-aminocarbazole is summarized in Figure 12. These multi-mode fluorescence switchability based on a relatively simple molecular framework should encourage further development of bioimaging materials and other luminescence applications.

EXPERIMENTAL SECTION

General. Unless otherwise noted, all reactions were carried out in well cleaned glasswares with magnetic stirring. Operations were performed under an atmosphere of dry argon using Schlenk and vacuum techniques, unless otherwise noted. All starting materials were obtained from commercial sources or were synthesized using standard procedures. Melting points were measured on a Yanaco MP-500D and are not corrected. ^{1}H and ^{13}C NMR spectra (400 and 100 MHz, respectively) were recorded on a Bruker Avance III HD 400 using TMS (0 ppm), and $CDCl_3$ (77.16 ppm) or $(CD_3)_2CO$ (29.84 ppm) as an internal standard, respectively. The following abbreviations are used in connection with NMR; s = singlet, d = doublet, t = triplet, q = quartet, quin = quintet, sep = septet, and m = multiplet. Mass spectra were measured using a JEOL JMS-T100LP (DART method, ambient ionization). Preparative column chromatography was performed using Kanto Chemical silica gel 60 N (spherical, neutral), Fuji Silysia BW-4:10MH silica gel or YMC_GEL Silica (6 nm I-40-63 um). Thin layer chromatography (TLC) was carried out on Merck 25 TLC silica gel 60 F_{254} aluminium sheets. Single crystal X-ray diffraction analyses were conducted using Bruker Apex-II diffractometer equipped with a CCD detector. Powder X-ray di□raction (XRD) patterns were obtained with a di□ractometer (Rigaku, SmartLab) using Cu Kα radiation. Steady state photoluminescence spectra of liquid samples were recorded on a spectrofluorometer (JASCO FP-8300) with a 1-cm-square quartz fluorescence cuvette. Steady state photoluminescence spectra of solid samples were recorded on a spectrofluorometer (JASCO FP-6600) with a quartz fluorescence cuvette and integrating sphere (Otsuka Electronics QE-2000). UV–visible spectra were recorded on a Shimadzu UV-1800 spectrometer and a JASCO V-770 spectrometer with a 1-cm-square quartz absorption cuvette (light path: 1 cm). In order to estimate particle sizes, DLS experiments were performed using Zetasizer Nano-S (Malvern Instruments, Worcestershire, UK). FE-SEM images were obtained using a JEOL JSM-7100F thermal field emission electron microscope instrument operated at 5.0 kV unless otherwise noted. The specimens for FE-SEM were prepared by placing a drop of the solution on N-type silicon wafer (thickness: 0.5 mm, orientation: <1 0 0>, resistivity: 8–12 Ohm cm) and drying under vacuum overnight. AFM images were obtained in dynamic mode using NanoNavi II/IIe and SPA-400 (Hitachi High-Tech Science Corporation, Tokyo, Japan) equipped with an OMCL-AC160TS-C3 micro cantilever (Olympus Corporation, Tokyo, Japan). The specimens for AFM were prepared by placing a drop of the solution on a cleaved mica plate and drying under vacuum overnight.

3,6-Dibromo-9-benzylcarbazole (10) To a solution of 3,6-dibromocarbazole (5.00 g, 15.4 mmol, 1.0 equiv) and potassium carbonate (21.3 g, 154 mmol, 10 equiv) in DMF (69 mL) was added benzyl bromide (3.7 mL, 30.8 mmol, 2.0 equiv) and the reaction mixture was stirred for 3 h at room temperature (rt). The reaction was quenched by being poured into 250 mL of ice water. A mixture was filtered and the solid was triturated and stirred in hexane (200 mL). The suspension was filtrated to afford the title product (4.51 g, 71% yield) as a white solid. Mp: 162.4–162.7 °C; ^{1}H NMR (400 MHz, $CDCl_3$): δ = 8.17 (d, *J* = 1.6 Hz, 2H), 7.52 (dd, *J* = 8.4, 2.0 Hz, 2H), 7.28–7.22 (m, 5H), 7.04 (dd, *J* = 6.4, 2.4 Hz, 2H), 5.46 (s, 2H) ppm; ^{13}C NMR (100 MHz, $CDCl_3$): δ = 139.6, 136.3, 129.4, 129.0, 127.9, 126.3, 123.7, 123.4, 112.6, 110.8, 46.8 ppm; IR (neat): ν = 3401, 3049, 1694, 1621, 1599, 1574, 1467, 1444, 1332, 1269, 1238, 1200, 1133, 1110, 1054, 1018, 1003, 928, 879, 843, 809, 766, 756, 745, 723, 678 cm^{-1}; HRMS (DART): m/z calcd for $C_{19}H_{14}{}^{79}Br^{81}BrN$: 415.9473 $[M+H^+]$; found: 415.9446.

3,6-Bis(dimethylamino)-9-benzylcarbazole (12) A solution of $Pd_2(dba)_3$ (100 mg, 0.109 mmol, 1.0 mol%) and Ruphos (120 mg, 0.257 mmol, 2.4 mol%) in THF (50 mL) was stirred for 30 min. To the solution were added 3,6-dibromo-9-benzylcarbazole (4.50 g, 10.8 mmol, 1.0 equiv), LiHMDS in *n*-hexane (1.17 M, 55.6 mL, 65.0 mmol, 6.0 equiv), THF (50 mL) and dimethylamine hydrochloride (2.66 g, 32.6 mmol, 3.0 equiv). The mixture was stirred for 5 h at 80 °C then cooled to rt. The reaction was quenched by adding 1 M HCl aq. (65 mL) then 20 mL of sat. $NaHCO_3$ aq. (20 mL). Ethyl acetate was added and the mixture was washed with water three times, dried over anhydrous Na_2SO_4, filtered, and concentrated in vacuo. The residue was purified by recrystallization in hexane/ethyl acetate to afford the title product (3.08 g, 83% yield) as a green solid. Mp: 212.8–213.4 °C; ^{1}H NMR (400 MHz, $(CD_3)_2CO$)): δ = 7.55 (d, *J* = 2.0 Hz, 2H), 7.33 (d, *J* = 8.8 Hz, 2H), 7.27–7.19 (m, 3H), 7.55 (dd, *J* = 7.2, 1.6 Hz, 2H), 7.02 (dd, *J* = 9.0, 2.4 Hz, 2H), 5.51 (s, 2H), 2.94 (s, 12H) ppm; ^{13}C NMR (100 MHz, $(CD_3)_2CO$): δ =146.2, 139.6, 135.9, 129.3, 127.9, 127.5, 124.4, 115.7, 110.2, 105.5, 46.8, 42.7 ppm; IR (neat): ν = 2873, 2797, 1615, 1572, 1493, 1480, 1450, 1436, 1340, 1327, 1264, 1213, 1167, 1142, 1122, 1056, 1029, 965, 949, 903, 842, 823, 793, 779, 751, 737, 721, 695, 650 cm^{-1}; HRMS (DART): m/z calcd for $C_{23}H_{26}N_3$: 344.2127 $[M+H^+]$; found: 344.2155.

3,6-Dibromo-9-(4-methoxybenzyl)carbazole (11) Sodium hydride (60% in mineral oil, 1.818 g, 45.52 mmol, 1.5 equiv) was washed using 20 mL of hexane, then the solution of 3,6-dibromocarbazole (9.625 g, 29.62 mmol, 1.0 equiv) in 60 mL of dimethylformamide (DMF) was added. To the solution was added *p*-methoxybenzylchloride (6.1 mL, 44.4 mmol, 1.5 equiv) and the solution was stirred for 3 h at rt. The reaction was quenched by adding water (70 mL). To the resultant mixture was added ethyl acetate and the organic layer was washed with brine six times, dried over anhydrous Na_2SO_4, filtered, and concentrated in vacuo. To the residue was added hexane (100 mL) and the mixture was stirred for 2 h, then filtered to afford the title product (13.15 g, >99% yield) as a white solid. Mp: 155.7–156.1 °C; ^{1}H NMR (400 MHz, $CDCl_3$): δ = 8.15 (d, *J* = 8.8 Hz, 2H), 7.51 (dd, *J* = 8.8, 2.0 Hz, 2H), 7.23 (d, *J* = 8.4 Hz, 2H), 7.00 (d, *J* = 8.8 Hz, 2H), 6.79 (d, *J* = 9.6 Hz, 2H), 5.39 (s, 2H), 3.74 (s, 3H) ppm; ^{13}C NMR (100 MHz, $CDCl_3$): δ = 159.2, 139.5, 129.3, 128.3, 127.7, 123.7, 123.4, 114.4, 112.4, 110.8, 55.4, 46.3 ppm; IR (neat): ν = 2934, 2835, 1611, 1587, 1512, 1469, 1448, 1433, 1374, 1334, 1314, 1302, 1289, 1246, 1203, 1176, 1145, 1112, 1059, 1033, 1017, 977, 887, 878, 846, 828, 815, 796, 788, 757, 737, 708, 648, 635 cm^{-1}; HRMS (DART): m/z calcd for C_8H_9O: 121.0653 $[(MeO)C_6H_4CH_2^+]$; found: 121.0629.

3,6-Bis(dimethylamino)-9-(4-methoxybenzyl)carbazole (13) A solution of $Pd_2(dba)_3$ (273 mg, 0.298 mmol, 1.0 mol%) and Ruphos (335 mg, 0.718 mmol, 2.4 mol%) in THF (100 mL) was stirred for 30 min. To the solution were added 3,6-dibromo-

9-(4-methoxybenzyl)carbazole (13.15 g, 29. 62 mmol, 1.0 equiv), LiHMDS (29.72 g, 177.6 mmol, 6.0 equiv), THF (200 mL) and dimethylamine hydrochloride (7.332 g, 89.92 mmol, 3.0 equiv). The mixture was stirred for 28 h at 80 °C then cooled to rt. The reaction was quenched by adding 1 M HCl aq. (178 mL) then sat. $NaHCO_3$ aq. (178 mL). To the solution was added ethyl acetate and the mixture was washed with brine six times, dried over anhydrous Na_2SO_4, filtered, and concentrated in vacuo to afford the title product (10.70 g, 97% yield) as a yellow solid. Mp: 144.5–145.0 °C; ^{1}H NMR (400 MHz, $CDCl_3$): δ = 7.54 (d, *J* = 2.4 Hz, 2H), 7.32 (d, 8.8 Hz, 2H), 7.09 (d, *J* = 8.8 Hz, 2H), 7.02 (dd, *J* = 8.8, 2.4 Hz, 2H), 6.79 (d, *J* = 8.8 Hz, 2H), 5.42 (s, 2H), 3.70 (s, 3H), 2.94 (s, 12H) ppm; ^{13}C NMR (100 MHz, $(CD_3)_2CO$): δ = 159.8, 146.0, 136.0, 131.3, 128.7, 124.4, 115.7, 114.6, 110.3, 105.5, 55.4, 46.3, 42.7 ppm; IR (neat): ν = 2795, 1613, 1572, 1499, 1482, 1435, 1327, 1297, 1246, 1214, 1172, 1137, 1109, 1055, 1029, 965, 948, 845, 820, 808, 786, 775, 754, 731, 666, 650, 634 cm^{-1}; HRMS (DART): m/z calcd for $C_{24}H_{28}N_3O$: 374.2232 [M+H$^+$]; found: 374.2253.

3,6-Bis(dimethylamino)-9H-carbazole (14)[20] To a solution of 3,6-dimethylamino-9-(4-methoxybenzyl)carbazole (100 mg, 0.268 mmol, 1.0 equiv) in CH_2Cl_2 (2.1 mL) was dropwise added over 5 minutes a solution of 1M BCl_3 in heptane (1.61 mL, 1.61 mmol, 6.0 equiv) at –78 °C and the mixture was stirred for 30 min, then stirred for 1 h at –20 °C. The solution was stirred for 90 h at rt with protection from light. The reaction was quenched by adding methanol (5.2 mL), and concentrated in vacuo. To the solid residue was added 4 M HCl aq. (9 mL) and the mixture was stirred at 70 °C. The resultant mixture was cooled to rt. 4 M NaOH aq. (20 mL) was added to basify the mixture. The resultant mixture was extracted with CH_2Cl_2 three times. The organic layer was dried over anhydrous Na_2SO_4, filtered, concentrated in vacuo. The residue was purified by column chromatography on NH_2-silica gel (hexane/ ethyl acetate = 1/ 1) to afford the title product (58 mg, 86% yield) as a green yellow solid.

3,6-Bis(dimethylamino)-9-(4-cyanophenyl)carbazole (1) A solution of 3,6-bis(dimethylamino)-9*H*-carbazole (285 mg, 1.13 mmol, 1.0 equiv), 4-iodobenzonitrile (285 mg, 1.24 mmol, 1.1 equiv), LiCl (48 mg, 1.1 mmol, 1.0 equiv), CuI (23 mg, 0.12 mmol, 10 mol%), 1,10-phenanthroline monohydrate (23 mg, 0.12 mmol, 10 mol%) and Cs_2CO_3 (485 mg, 1.49 mmol, 1.3 equiv) in DMF (5.0 mL) was stirred for 19 h at 150 °C. After cooled to rt, the reaction was quenched by adding NH_4Cl aq. (17 mL). Ethyl acetate was added and the mixture was washed with brine seven times, dried over anhydrous Na_2SO_4, filtered and concentrated in vacuo. The residue was purified by column chromatography on silica gel (hexane/ethyl acetate = 3/1) to afford the title product (258 mg, 65% yield) as a yellow solid. Single crystals of **1** suitable for X-ray diffraction analysis were obtained by recrystallization from hexane/1,2-dichloroethane by vapor diffusion. Mp: 254.8–255.2 °C. ^{1}H NMR (400 MHz, $CDCl_3$): δ = 7.83 (d, *J* = 8.4 Hz, 2H), 7.70 (d, *J* = 8.4 Hz, 2H), 7.41 (s, 2H), 7.39 (d, *J* = 9,0 Hz, 2H), 6.99 (dd, *J* = 9.0, 2.4 Hz, 2H), 3.04 (s, 12H) ppm; ^{13}C NMR (100 MHz, $CDCl_3$): δ = 146.6, 143.2, 133.8, 133.7, 125.8, 125.3, 118.9, 114.8, 110.3, 108.6, 104.4, 42.5 ppm; IR(neat): ν = 2840, 2792, 2216, 1603, 1578, 1512, 1498, 1471, 1435, 1372, 1329, 1218, 1171, 1148, 1132, 1106, 1061, 968, 947, 910, 858, 826, 798, 748, 716, 661, 643, 602 cm^{-1}. HRMS(DART) = m/z calcd for $C_{23}H_{23}N_4$: 355.1923 [M+H$^+$]; found: 355.1904.

Methyl 4-[3,6-bis(dimethylamino)carbazol-9-yl]benzoate (2) A solution of 3,6-bis(dimethylamino)-9*H*-carbazole (300 mg, 1.18 mmol, 1.0 equiv), methyl 4-iodobenzoate (342 mg, 1.31 mmol, 1.1 equiv), LiCl (52 mg, 1.2 mmol, 1.0 equiv), CuI (26 mg, 0.14 mmol, 10 mol%), 1,10-phenanthroline (25 mg, 0.13 mmol, 10 mol%) and Cs_2CO_3 (464 mg, 1.42 mmol, 1.2 equiv) in DMF (5.0 mL) was stirred for 12 h at 150 °C. After cooled to rt, the reaction was quenched by adding NH_4Cl aq. (17 mL). Ethyl acetate was added and the solution was washed with brine five times, dried over anhydrous Na_2SO_4, filtered and concentrated in vacuo. The residue was purified by column chromatography on silica gel (hexane/ethyl acetate = 1/1) to afford the title product (294 mg, 64% yield) as a yellow solid. Mp 146.4–146.9 °C; ^{1}H NMR (400 MHz, $CDCl_3$): δ = 8.23 (dt, *J* = 8.8, 1.9 Hz, 2H), 7.66 (dt, *J* = 8.8, 2.1 Hz, 2H), 7.44 (d, *J* = 2.4 Hz, 2H), 7.43 (d, *J* = 8.8 Hz, 2H), 7.01 (dd, *J* = 9.0, 2.6 Hz, 2H), 3.97 (s, 3H) 3.03 (s, 12H) ppm; ^{13}C NMR (100 MHz, $CDCl_3$): δ = 166.7, 146.3, 143.1, 134.2, 131.3, 127.2, 125.3, 124.9, 115.0, 110.4, 104.5, 52.4, 42.6 ppm; IR (neat): ν = 2988, 2937, 2874, 2842, 2791, 1707, 1606, 1573, 1496, 1473, 1433, 1348, 1326, 1277, 1220, 1190, 1173, 1106, 950, 817, 797, 782, 769, 703, 584 cm^{-1}; HRMS (DART): m/z calcd for $C_{24}H_{26}N_3O_2$: 388.2025 [M+H$^+$]; found: 388.2010.

3,6-Bis(dimethylamino)-9-phenylcarbazole (3) A solution of 3,6-bis(dimethylamino)-9*H*-carbazole (300 mg, 1.18 mmol, 1.0 equiv), bromobenzene (1.24 mL, 11.8 mmol, 10 equiv), CuI (237 mg, 1.24 mmol, 1.05 equiv), K_2CO_3 (639 mg, 4.62 mmol, 3.9 equiv) in dimethyl acetoamide (DMA, 6 mL) was stirred for 18 h at 180 °C with protection from light. The reaction was quenched by being poured into water (100 mL). Conc. NH_3 aq. was added and the mixture was extracted with CH_2Cl_2 three times. The organic layer was washed with brine three times, dried over anhydrous Na_2SO_4, filtered. The filtrate was concentrated in vacuo and purified by column chromatography on silica gel (hexane/ethyl acetate = 1/1) to give the product (295 mg, 76% yield) as a brown oil. ^{1}H NMR (400 MHz, $CDCl_3$): δ = 7.57 (d, *J* = 4.4 Hz, 4H), 7.51 (d, *J* = 2.4 Hz, 2H), 7.42–7.40 (m, 1H), 7.37 (d, *J* = 8.8 Hz, 2H), 7.04 (dd, *J* = 9.2, 2.4 Hz, 2H), 3.04 (s, 12H) ppm; ^{13}C NMR (100 MHz, $CDCl_3$): δ = 145.8, 138.7, 135.3, 129.8, 126.5, 126.5, 124.2, 115.3, 110.3, 104.8, 42.9 ppm; IR (neat): ν = 2842, 2794, 1618, 1591, 1573, 1486, 1475, 1435, 1354, 1325, 1280, 1220, 1165, 1148, 1110, 1079, 1056, 1024, 968, 949, 908, 894, 860, 836, 816, 795, 783, 761, 739, 715, 700, 666, 659, 631, 616 cm^{-1}; HRMS (DART): m/z calcd for $C_{22}H_{24}N_3$: 330.1970 [M+H$^+$]; found: 330.1997.

3-Bromo-9H-carbazole (15)[39] A solution of carbazole (1.00 g, 6.00 mmol, 1.0 equiv) in THF (12 mL) was cooled in ice bath. To the mixture was added *N*-bromosuccinimide (1.07 g, 6.00 mmol, 1.0 equiv) slowly with protection from light. After stirring for 30 min at 0 °C, the solution was stirred for 17 h at rt. The reaction was quenched by adding sat. Na_2SO_3 aq. (10 mL) and the solution was concentrated in vacuo to remove THF. Ethyl acetate was added and the solution was washed with brine four times, dried over anhydrous Na_2SO_4, filtrate and concentrated in vacuo to afford the title product (1.31 g, 89% yield) as a white solid.

3-Dimethylamino-9H-carbazole (16) A solution of $Pd_2(dba)_3$ (11 mg, 12 μmol, 1.0 mol%) and Ruphos (14 mg, 30 μmol, 2.4 mol%) in THF (13.2 mL) was stirred. To the solution were added 3-bromo-9*H*-carbazole (300 mg, 1.22 mmol, 1.0 equiv), LiHMDS (1.22 g, 7.31 mmol, 6.0 equiv) and dimethylamine hydrochloride (297 mg, 3.64 mmol, 3.0 equiv). The mixture was stirred for 65 h at 120 °C then cooled to rt. The reaction

was quenched by adding 1 M HCl aq. (7.3 mL) then sat. $NaHCO_3$ aq. (7.3 mL). Ethyl acetate was added and the solution was washed with brine three times, dried over anhydrous Na_2SO_4, filtered, concentrated in vacuo. Another two sets of reactions were conducted under the same conditions. The obtained crude materials were combined and purified by column chromatography on silica gel (hexane/ ethyl acetate) to afford the title product (563 mg, 73% yield) as a green yellow solid. Mp: 114.7–115.0 °C; ^{1}H NMR (400 MHz, $(CD_3)_2CO$): δ = 9.97 (s, 1H), 8.07 (dd, *J* = 7.8, 1.2 Hz, 1H), 7.54 (d, *J* = 2.4 Hz, 1H), 7.44 (d, *J* = 8.4 Hz, 1H), 7.39 (d, *J* = 8.4 Hz, 1H), 7.33 (td, *J* = 7.4, 1.2 Hz, 1H), 7.11 (td, *J* = 7.4, 0.8 Hz, 1H), 7.06 (dd, *J* = 8.8, 2.4 Hz, 1H), 2.97 (s, 6H) ppm; ^{13}C NMR (100 MHz, $(CD_3)_2CO$): δ = 146.5, 141.6, 134.6, 125.9, 124.6, 124.1, 120.8, 118.8, 116.0, 111.9, 111.5, 105.0, 42.6 ppm; IR (neat): ν = 3025, 2948, 2863, 2835, 2788, 1609, 1585, 1496, 1484, 1471, 1450, 1435, 1328, 1306, 1276, 1241, 1184, 1158, 1135, 1105, 1045, 1019, 1007, 946, 934, 888, 870, 848, 804, 767, 751, 735, 714, 637, 613 cm^{-1}; HRMS (DART): m/z calcd for $C_{14}H_{15}N_2$: 211.1235 [M+H$^+$]; found: 211.1242.

***3-Dimethylamino-9-(4-cyanophenyl)carbazole* (4)** A solution of 3-dimethylamino-9*H*-carbazole (250 mg, 1.19 mmol, 1.0 equiv), 4-iodobenzonitrile (300 mg, 1.31 mmol, 1.1 equiv), LiCl (50 mg, 1.18 mmol, 1.0 equiv), CuI (23 mg, 0.12 mmol, 10 mol%), 1,10-phenanthroline monohydrate (24 mg, 0.12 mmol, 10 mol%) and Cs_2CO_3 (504 mg, 1.55 mmol, 1.3 equiv) in DMF (5.3 mL) was stirred for 41 h at 150 °C. After cooled to rt, the reaction was quenched by adding NH_4Cl aq. (17 mL). Ethyl acetate was added and the solution was washed with brine five times, dried over anhydrous Na_2SO_4, filtered and concentrated in vacuo. The residue was purified by column chromatography on silica gel (hexane/ethyl acetate = 3/1) to afford the title product (247 mg, 67% yield) as a yellow solid. Mp: 134.3–135.2 °C; ^{1}H NMR (400 MHz, $CDCl_3$): δ = 8.09 (d, *J* = 7.4 Hz, 2H), 7.87 (d, *J* = 8.8 Hz, 2H), 7.73 (d, *J* = 8.8 Hz, 2H), 7.47 (d, *J* = 2.4 Hz, 1H), 7.46 (d, *J* = 8.0 Hz, 1H), 7.42–7.36 (m, 2H), 7.28 (dt, *J* = 1.2, 7.4 Hz, 1H), 7.02 (dd, *J* = 8.8, 2.4 Hz, 1H), 3.04 (s, 6H) ppm; ^{13}C NMR (100 MHz, $CDCl_3$): δ = 146.9, 142.7, 140.2, 133.9, 133.3, 126.5, 126.2, 125.0, 124.4, 120.6, 118.7, 114.8, 110.2, 109.6, 104.2, 42.3 ppm; IR (neat): ν = 3048, 2840, 2796, 2222, 1667, 1626, 1599, 1497, 1454, 1440, 1367, 1328, 1296, 1225, 1173, 1151, 1132, 1104, 1067, 1028, 955, 914, 842, 831, 795, 761, 744, 735, 665, 631, 620 cm^{-1}; HRMS (DART): m/z calcd for $C_{21}H_{18}N_3$: 312.1501 [M+H$^+$]; found: 312.1523.

***3-Dimethylamino-9-phenylcarbazole* (5)** A solution of 3-dimethylamino-9-carbazole (200 mg, 0.95 mmol, 1.0 equiv), bromobenzene (1.00 mL, 9.55 mmol, 10 equiv), CuI (195 mg, 1.02 mmol, 1.07 equiv), K_2CO_3 (513 mg, 3.71 mmol, 3.9 equiv) in DMA (4.8 mL) was stirred for 18 h at 180 °C with protection from light. After cooled to rt, the reaction was quenched by being poured into water (240 mL). Conc. NH_3 aq. was added and the solution was extracted with CH_2Cl_2 five times. The organic layer was concentrated in vacuo in order to remove CH_2Cl_2. Ethyl acetate was added and the organic layer was washed with brine five times, dried over anhydrous Na_2SO_4, filtered. The filtrate was concentrated in vacuo and purified by column chromatography on silica gel (hexane/ethyl acetate = 10/1) to give the product (218 mg, 80% yield). ^{1}H NMR (400 MHz, $CDCl_3$): δ = 8.11 (d, *J* = 7.6 Hz, 1H), 7.61–7.56 (m, 4H), 7.53 (d, *J* = 2.4 Hz, 1H), 7.45–7.40 (m, 2H), 7.38 (td, *J* = 6.8, 1.2 Hz, 1H), 7.35 (d, *J* = 6.8 Hz, 1H), 7.24 (td, *J* = 7.4, 1.2 Hz, 1H), 7.05 (dd, *J* = 2.4, 8.8 Hz, 1H), 3.03 (s, 6H) ppm; ^{13}C NMR (100 MHz, $CDCl_3$): δ = 146.3, 141.2, 138.3, 134.8, 129.9, 127.0, 126.9, 125.8, 124.1, 123.5, 120.3, 119.4, 115.3, 110.3, 109.8, 104.7, 42.7 ppm; IR (neat): ν = 2788, 1673, 1594, 1492, 1451, 1438, 1363, 1326, 1228, 1134, 1103, 1074, 1025, 953, 926, 835, 794, 759, 741, 697, 684, 643, 619 cm^{-1}; HRMS (DART): m/z calcd for $C_{20}H_{19}N_2$: 287.1548 [M+H$^+$]; found: 287.1548.

9-(4-Cyanophenyl)carbazole (6)[40] A solution of 9*H*-carbazole (837 mg, 5.00 mmol, 1.0 equiv), 4-iodobenzonitrile (1.260 g, 5.50 mmol, 1.1 equiv), LiCl (212 mg, 5.50 mmol, 1.0 equiv), CuI (96 mg, 0.50 mmol, 10 mol%), 1,10-phenanthroline monohydrate (99 mg, 0.50 mmol, 10 mol%) and Cs_2CO_3 (2.120 g, 6.51 mmol, 1.3 equiv) in DMF (20.5 mL) was stirred for 22 h at 150 °C. The reaction was quenched by adding sat. NH_4Cl aq. (20.5 mL). Ethyl acetate was added and the organic layer was washed with brine five times and sat. NH_4Cl aq. four times, dried over anhydrous Na_2SO_4, filtered and concentrated in vacuo to afford the title product (1.329 g, 99% yield) as a white solid.

3,6-Dimethoxy-9-(4-cyanophenyl)carbazole (7) A solution of 3,6-dimethoxy-9*H*-carbazole (455 mg, 2.00 mmol, 1.0 equiv), 4-iodobenzonitrile (504 mg, 2.20 mmol, 1.1 equiv), CuI (38 mg, 0.20 mmol, 10 mol%), LiCl (85 mg, 2.00 mmol, 1.0 equiv), 1,10-phenanthroline monohydrate (40 mg, 0.20 mmol, 10 mol%) and Cs_2CO_3 (847 mg, 2.60 mmol, 1.3 equiv) in DMF (8.2 mL) was stirred for 21 h at 150 °C. The reaction was quenched by adding sat. NH_4Cl aq. (8.2 mL). Ethyl acetate was added and the organic layer was washed with sat. NH_4Cl aq. four times and brine three times, dried over anhydrous Na_2SO_4, filtered and concentrated in vacuo. The residue was purified by column chromatography on silica gel (hexane/ethyl acetate = 5/1) to afford the title product (508 mg, 77% yield) as a white solid. Mp: 173.6–173.8 °C; ^{1}H NMR (400 MHz, $CDCl_3$): δ = 7.87 (d, *J* = 8.8 Hz, 2H), 7.70 (d, *J* = 8.8 Hz, 2H), 7.54 (d, *J* = 2.4 Hz, 2H), 7.39 (d, *J* = 8.8 Hz, 2H), 7.05 (dd, *J* = 8.8, 2.4 Hz, 2H), 3.95 (s, 6H) ppm; ^{13}C NMR (100 MHz, $CDCl_3$): δ = 154.8, 142.6, 135.1, 134.0, 126.4, 124.6, 118.6, 115.5, 110.7, 109.7, 103.2, 56.1 ppm; IR(neat): ν = 2988, 2953, 2933, 2828, 2226, 1626, 1601, 1506, 1488, 1462, 1449, 1428, 1371, 1328, 1291, 1263, 1202, 1184, 1175, 1160, 1111, 1040, 1028, 957, 943, 910, 849, 810, 824, 793, 749, 726, 663, 641, 605 cm^{-1}; HRMS(DART) = m/z calcd for $C_{21}H_{17}N_2O_2$: 329.1290 [M+H$^+$]; found: 329.1308.

3-Nitro-9-(4-cyanophenyl)carbazole (17) A solution of 9-(4-cyanophenyl)carbazole (531 mg, 2.00 mmol, 1.0 equiv) in AcOH (3.5 mL) was stirred. To the solution was added nitric acid (1.50 mL, 33.8 mmol, 17 equiv). The mixture was stirred for 1 hour at rt. The mixture was cooled in ice bath and the suspension was filtrated, washed with ice-cooled distilled water thirty times. The remaining water of the obtained solids was removed with papers to give the crude material (528 mg, 72%). The yield was determined by ^{1}H NMR analysis with durene as an internal standard. Mp: 256.2–256.6 °C; ^{1}H NMR (400 MHz, $CDCl_3$): δ = 9.07 (d, *J* = 2.4 Hz, 1H), 8.35 (dd, *J* = 8.8 Hz, 1H), 8.23 (dd, *J* = 7.2, 1.6 Hz, 1H), 7.99 (d, *J* = 8.8 Hz, 2H), 7.75 (d, *J* = 8.8 Hz, 2H), 7.56 (dt, *J* = 1.2, 8.0 Hz, 1H), 7.47–7.42 (m, 3H) ppm; ^{13}C NMR (100 MHz, $CDCl_3$): δ = 143.2, 142.2, 141.5, 140.7, 134.4, 128.2, 127.7, 123.9, 123.5, 122.6, 122.3, 121.4, 118.0, 117.5, 112.3, 110.5, 109.5 ppm; IR (neat): ν = 3085, 2227, 1601, 1584, 1505, 1471, 1448, 1334, 1286, 1270, 1242, 1224, 1186, 1166, 1113, 1088, 1022, 915, 893, 860, 847, 835, 817, 788, 767, 746, 727, 718, 703, 658, 636, 623 cm^{-1}; HRMS (DART): m/z calcd for $C_{19}H_{12}N_3O_2$: 314.0930 [M+H$^+$]; found: 314.0943.

3-Amino-9-(4-cyanophenyl)carbazole (18) A mixture of the crude material of 3-nitro-9-(4-cyanophenyl)carbazole obtained above (366 mg, purity 86%, 1.0 mmol, 1.0 equiv) and 10wt% Pd/C (106 mg, 0.10 mmol, 10 mol%) in MeOH (10 mL) was stirred under hydrogen gas (1 atm). After 7 h, the reactant mixture was filtrated on celite. After the concentration of the filtrate, the residue was purified by chromatography on silica gel (hexane/ ethyl acetate = 1/ 3) to afford the title product as a white solid (93 mg, 33%). Mp: 176.0–176.7 °C; ^{1}H NMR (400 MHz, $CDCl_3$): δ = 8.03 (d, *J* = 7.6 Hz, 1H), 7.86 (d, *J* = 8.8 Hz, 2H), 7.70 (d, *J* = 8.8 Hz, 2H), 7.45 (d, *J* = 8.0 Hz, 1H), 7.43 (d, *J* = 2.0 Hz, 1H), 7.39 (td, *J* = 8.4, 1.2 Hz, 1H), 7.29 (d, *J* = 6.0 Hz, 1H), 7.27 (dt, *J* = 1.2, 7.2 Hz, 1H), 6.85 (dd, *J* = 8.6, 2.4 Hz, 1H), 3.70 (s, 2H) ppm; ^{13}C NMR (100 MHz, $CDCl_3$): δ = 142.5, 141.0, 140.2, 134.0, 133.9, 126.6, 126.3, 125.1, 123.9, 120.6, 120.6, 118.7, 115.8, 110.4, 109.7, 109.6, 106.0 ppm; IR (neat): ν = 3384, 3197, 2223, 1626, 1599, 1511, 1491, 1454, 1361, 1338, 1317, 1235, 1207, 1169, 1025, 936, 911, 884, 864, 856, 826, 806, 765, 742, 718, 700, 646, 632, 609, 600 cm^{-1}; HRMS (DART): m/z calcd for $C_{19}H_{14}N_3$: 284.1188 [M+H$^+$]; found: 284.1202.

4-(2,3,6,7-Tetrahydro-1H-quinolizino[1,9-bc]carbazol-9(5H)-yl)benzonitrile (8) A mixture of 3-amino-9-(4-cyanophenyl)carbazole (57 mg, 0.20 mmol, 1.0 equiv) and Na2CO3 (85 mg, 0.80 mmol, 4.0 equiv) in 1-bromo-3-chloropentane (0.3 mL, 3.05 mmol, 15 equiv) was stirred for 1 h at 70 °C, then for 24 h at 100 °C. The reaction was cooled to rt. To the reactant mixture were added CH_2Cl_2 and water and the mixture was extracted with CH_2Cl_2 three times, dried over anhydrous Na_2SO_4, filtered. The filtrate was concentrated in vacuo. To the crude material was added DMF (2 mL). The mixture was stirred for 90 h at 160 °C. The reaction was cooled to rt. Ethyl acetate was added and the mixture was washed with brine eight times, dried over anhydrous Na_2SO_4, filtered and concentrated in vacuo. The residue was purified by chromatography on silica gel to afford the title product as a yellow amorphous (19 mg, 26% yield). ^{1}H NMR (400 MHz, $CDCl_3$): δ = 8.13 (d, *J* = 7.6 Hz, 1H), 7.87 (d, *J* = 8.4 Hz, 2H), 7.69 (d, *J* = 8.4 Hz, 2H), 7.41 (d, *J* = 8.0 Hz, 1H), 7.34 (t, *J* = 7.2 Hz, 1H), 7.23 (t, *J* = 7.2 Hz, 1H), 6.97 (s, 1H), 3.40 (t, *J* = 6.8 Hz, 2H), 3.19–3.12 (m, 4H), 2.94 (t, *J* = 6.8 Hz, 2H), 2.23 (quin, *J* = 6.8 Hz, 2H), 2.06 (quin, *J* = 6.4 Hz, 2H) ppm; ^{13}C NMR (100 MHz, $CDCl_3$): δ = 142.7, 140.2, 139.1, 133.9, 133.1, 127.2, 125.1, 123.5, 123.1, 121.1, 120.3, 118.7, 117.2, 109.8, 109.1, 107.4, 51.2, 50.5, 29.0, 26.1, 22.7, 22.6 ppm; IR (neat): ν = 3053, 2929, 2837, 2221, 1599, 1507, 1487, 1479, 1466, 1450, 1437, 1425, 1398, 1366, 1327, 1315, 1293, 1270, 1241, 1215, 1201, 1186, 1175, 1155, 1117, 1086, 1070, 1055, 1028, 959, 929, 916, 886, 858, 843, 836, 795, 769, 743, 726, 682, 666, 654, 631, 618 cm^{-1}; HRMS (DART): m/z calcd for $C_{25}H_{22}N_3$: 364.1814 [M+H$^+$]; found: 364.1805.

3,6-Bis(dimethylamino)-9-(4-formylphenyl)carbazole (20) A solution of 3,6-bis(dimethylamino)-9*H*-carbazole (900 mg, 3.55 mmol, 1.0 equiv), 4-iodobenzaldehyde (907 mg, 3.91 mmol, 1.1 equiv), LiCl (157 mg, 4.28 mmol, 1.0 equiv), CuI (69.2 mg, 0.363 mmol, 10 mol%), 1,10-phenanthroline monohydrate (70.7 mg, 0.357 mmol, 10 mol%) and Cs_2CO_3 (1.34 g, 4.28 mmol, 1.2 equiv) in DMF (15 mL) was stirred for 5 h at 150 °C. The reaction was quenched by adding sat. NH_4Cl aq. (51 mL). Ethyl acetate was added and the mixture was washed with brine six times, dried over anhydrous Na_2SO_4, filtered and concentrated in vacuo to afford the title product (1.223 g, 96% yield) as a red solid. Mp: 192.3–193.3 °C; ^{1}H NMR (400 MHz, $CDCl_3$): δ = 10.06 (s, 1H), 8.07 (dt, *J* = 8.4, 2.0 Hz, 2H), 7.77 (dt, *J* = 8.8, 2.0 Hz, 2H), 7.46 (d, *J* = 9.2 Hz, 2H), 7.43 (d, *J* = 2.4 Hz, 2H), 7.00 (dd, *J* = 9.2, 2.4 Hz, 2H), 3.04 (s, 12H) ppm; ^{13}C NMR (100 MHz, $CDCl_3$): δ = 191.1, 146.5, 144.6, 133.9, 133.4, 131.5, 125.5, 125.2, 114.8, 110.5, 104.4, 42.5 ppm; IR (neat): ν = 2842, 2799, 1679, 1596, 1578, 1558, 1511, 1495, 1472, 1435, 1391, 1368, 1343, 1323, 1302, 1213, 1169, 1149, 1105, 1063, 965, 949, 909, 860, 831, 799, 787, 744, 727, 719, 677, 658, 631 cm^{-1}; HRMS (DART): m/z calcd for $C_{23}H_{24}N_3O$: 358.1919 [M+H$^+$]; found: 358.1949.

3,6-Bis(dimethylamino)-9-[4-(1,3-thiazolidin-2-yl)phenyl]-9H-carbazole (21) A solution of 3,6-bis(dimethylamino)-9-(4-formylphenyl)carbazole (71.5 mg, 0.200 mmol, 1.0 equiv) and cysteamine (154 mg, 2.00 mmol, 10 equiv) in CH_3CN (8 mL) was stirred at rt for 20 h then at 40 °C for 29 h. The reaction was cooled to rt and quenched by adding brine and ethyl acetate. After concentration in vacuo, ethyl acetate was added and the mixture was washed by brine three times, dried over anhydrous Na_2SO_4, filtered and concentrated in vacuo. The residue was purified by column chromatography on silica gel (hexane/ethyl acetate = 1/3) to afford the title product (33 mg, 40% yield) as yellow oil. ^{1}H NMR (400 MHz, $CDCl_3$): δ = 7.68 (d, *J* = 8.4 Hz, 2H), 7.54 (d, *J* = 8.0 Hz, 2H), 7.47 (d, *J* = 2.4 Hz, 2H), 7.35 (d, *J* = 8.8 Hz, 2H), 7.01 (dd, *J* = 8.4, 2.4 Hz, 2H), 5.67 (s, 1H), 3.70–3.61 (m, 1H), 3.23–3.13 (m, 3H), 3.02 (s, 12H), 2.04 (s, 1H) ppm; ^{13}C NMR (100 MHz, $CDCl_3$): δ = 145.9, 138.6, 138.2, 135.1, 128.7, 126.3, 124.3, 115.3, 110.3, 104.7, 73.1, 53.0, 42.8, 36.8 ppm; IR (neat): ν = 2957, 2925, 2855, 1726, 1700, 1598, 1489, 1466, 1369, 1259, 1231, 1189, 1162, 1107, 1070, 1025, 960, 796, 753, 688 cm^{-1}; HRMS (DART): m/z calcd for $C_{23}H_{24}N_3O_1$: 358.1919 [M+H$^+$]; found: 358.1930. In the mass analysis only the ion peaks derived from compound **20** were observed instead of those of **21**, probably owing to the rapid hydrolysis under the ionization conditions.

Fluorescence spectra of 1 in the THF/water mixed solvents with various water fraction (Figure 3) Samples for fluorescence measurements in the THF/water mixed solvents were made as follows. In all cases the concentration of **1** was 10 μM. (a) 1 mM THF solution of **1** (**A**) 0.03 mL + THF 2.97 mL (f_w = 0) (b) **A** 0.03 mL + THF 2.67 mL + water 0.3 mL (f_w = 10) (c) **A** 0.03 mL + THF 2.07 mL + water 0.9 mL (f_w = 30) (d) **A** 0.03 mL + THF 1.47 mL + water 1.5 mL (f_w = 50) (e) **A** 0.03 mL + THF 0.87 mL + water 2.1 mL (f_w = 70) (f) **A** 0.03 mL + THF 0.27 mL + water 2.7 mL (f_w = 90) (g) **A** 0.03 mL + water 2.97 mL (f_w = 99). The sample preparation and fluorescence measurements were conducted under ambient atmosphere. Excitation light wavelength: 335 nm.

Solid sample preparation of 1 for comparison of as prepared microcrystal and ground powder (Figure 5) The microcrystal of NAC **1** was prepared according to the following recrystallization procedure. After purification by column chromatography, NAC **1** (258 mg) was dissolved in ethyl acetate (43 mL) and hexane (75 mL) at 60 °C, then the solution was cooled to –20 °C and left for overnight. The mixture was filtered and the solids were washed by the hexane/ethyl acetate (2/1) mixed solvents (10 mL) to afford the microcrystals of NAC **1** (174 mg). The powder material of NAC **1** was prepared by grinding the microcrystals with a pestle and mortar.

Fluorescence spectra of 1 in the THF/hexane mixed solvents with various hexane fraction (Figure 7) Samples for fluorescence measurements in the THF/hexane mixed solvents were made as follows. In all cases the concentration of **1** was

10 μM. (a) 0.5 mM THF solution of **1** (**B**) 0.06 mL + THF 2.94 mL ($f_h = 0$) (b) **B** 0.06 mL + THF 2.64 mL + hexane 0.3 mL ($f_h = 10$) (c) **B** 0.06 mL + THF 2.04 mL + hexane 0.9 mL ($f_h = 30$) (d) **B** 0.06 mL + THF 1.44 mL + hexane 1.5 mL ($f_h = 50$) (e) **B** 0.06 mL + THF 0.84 mL + hexane 2.1 mL ($f_h = 70$) (f) **B** 0.06 mL + THF 0.24 mL + hexane 2.7 mL ($f_h = 90$) (g) **B** 0.06 mL + hexane 2.94 mL ($f_h = 98$). The sample preparation and fluorescence measurements were conducted under ambient atmosphere. Excitation light wavelength: 335 nm.

Lipid droplet detection with Nile Red and NAC 1 (Figure 8) HeLa cells (Riken BioResource Center) were cultured in high glucose DME medium (Sigma-Aldrich) containing 10 %(v/v) FBS, 1 %(v/v) Penicillin-Streptomycin (P/S) (Sigma-Aldrich) at 37 °C in a CO_2 incubator (5% CO_2). Then, the HeLa cells were seeded at a density of 2×10^5 cells/mL in DME medium in a 35 mm glass bottom dish. After 24 hours of culture, to increase triacylglycerol synthesis and storage in cells, 62.5 μM oleic acid complexed to albumin (OA/BSA) was added to the medium and incubated overnight. To visualize LDs using dyes, the cells were incubated with 30-300 μM Nile Red and/or NAC **1** for 15 min in a CO_2 incubator (5 % CO_2) at 37 °C. After the incubation, the cells were washed thrice with PBS buffer. The fluorescence derived from Nile Red or NAC **1** was then analyzed using a fluorescence microscope (BZ-X700; KEYENCE) equipped with BZ-X filter TRITC or DAPI and a 40x objective lens with the exposure time indicated.

Fluorescence measurements of NAC 20 in the presence of cysteamine (Figure 9) Samples were made by adding the designated amount of 1 M aqueous solution of cysteamine to 25 mM CH_3CN solution of NAC **20** (1 mL) and stirring at 40 °C for 12 h. The amount of added cysteamine solution is as follows: (a) 2.5 μL (0.1 equiv) (b) 5.0 μL (0.2 equiv) (c) 7.5 μL (0.3 equiv) (d) 10 μL (0.4 equiv) (e) 12.5 μL (0.5 equiv) (f) 18.75 μL (0.75 equiv) (g) 25 μL (1.0 equiv). Each sample was diluted to 10 μM and subjected to fluorescence measurements. Excitation light wavelength: 335 nm, Slit width: 2.5 nm/2.5 nm, Sensibility: high, Under ambient atmosphere.

ASSOCIATED CONTENT

Supporting Information.
CIF file for NAC **1**, absorption and fluorescence spectra, experimental procedure for quantum yield determination, FE-SEM and AFM images, calculation details, X-ray crystallographic details and ^1H and ^{13}C NMR spectra (PDF)
This material is available free of charge via the Internet at http://pubs.acs.org.

REFERENCES

(1) de Silva, A. P.; Gunaratne, H. Q. N.; Gunnlaugsson, T.; Huxley, A. J. M.; McCoy, C. P.; Rademacher, J. T.; Rice, T. E., Signaling Recognition Events with Fluorescent Sensors and Switches. *Chem. Rev.* **1997,** *97*, 1515-1566.
(2) Callan, J. F.; de Silva, A. P.; Magri, D. C., Luminescent sensors and switches in the early 21st century. *Tetrahedron* **2005,** *61*, 8551-8588.
(3) Wiskur, S. L.; Ait-Haddou, H.; Lavigne, J. J.; Anslyn, E. V., Teaching Old Indicators New Tricks. *Acc. Chem. Res.* **2001,** *34*, 963-972.
(4) Klymchenko, A. S.; Mely, Y., Chapter Two - Fluorescent Environment-Sensitive Dyes as Reporters of Biomolecular Interactions. In *Prog. Mol. Biol. Transl. Sci.*, Morris, M. C., Ed. Academic Press: 2013; Vol. 113, pp 35-58.
(5) Han, J.; Burgess, K., Fluorescent Indicators for Intracellular pH. *Chem. Rev.* **2010,** *110*, 2709-2728.
(6) Förster, T.; Kasper, K., Ein Konzentrationsumschlag der Fluoreszenz. *Phys. Chem. (Muenchen, Ger.)* **1954,** *1*, 275-277.
(7) Birks, J. B., *Photophysics of Aromatic Molecules*. Wiley: New York, 1970.
(8) Mei, J.; Leung, N. L. C.; Kwok, R. T. K.; Lam, J. W. Y.; Tang, B. Z., Aggregation-Induced Emission: Together We Shine, United We Soar! *Chem. Rev.* **2015,** *115*, 11718-11940.
(9) He, Z.; Ke, C.; Tang, B. Z., Journey of Aggregation-Induced Emission Research. *ACS Omega* **2018,** *3*, 3267-3277.
(10) Luo, J.; Xie, Z.; Lam, J. W. Y.; Cheng, L.; Chen, H.; Qiu, C.; Kwok, H. S.; Zhan, X.; Liu, Y.; Zhu, D.; Tang, B. Z., Aggregation-induced emission of 1-methyl-1,2,3,4,5-pentaphenylsilole. *Chem. Commun.* **2001**, 1740-1741.
(11) Mei, J.; Hong, Y.; Lam, J. W. Y.; Qin, A.; Tang, Y.; Tang, B. Z., Aggregation□Induced Emission: The Whole Is More Brilliant than the Parts. *Adv. Mater.* **2014,** *26*, 5429-5479.
(12) Kang, X.; Wang, S.; Zhu, M., Observation of a new type of aggregation-induced emission in nanoclusters. *Chem. Sci.* **2018,** *9*, 3062-3068.
(13) Zheng, Z.; Zhang, T.; Liu, H.; Chen, Y.; Kwok, R. T. K.; Ma, C.; Zhang, P.; Sung, H. H. Y.; Williams, I. D.; Lam, J. W. Y.; Wong, K. S.; Tang, B. Z., Bright Near-Infrared Aggregation-Induced Emission Luminogens with Strong Two-Photon Absorption, Excellent Organelle Specificity, and Efficient Photodynamic Therapy Potential. *ACS Nano* **2018,** *12*, 8145-8159.
(14) Yeh, R.-H.; Yan, X.; Cammer, M.; Bresnick, A. R.; Lawrence, D. S., Real Time Visualization of Protein Kinase Activity in Living Cells. *J. Biol. Chem.* **2002,** *277*, 11527-11532.
(15) Parisio, G.; Marini, A.; Biancardi, A.; Ferrarini, A.; Mennucci, B., Polarity-Sensitive Fluorescent Probes in Lipid Bilayers: Bridging Spectroscopic Behavior and Microenvironment Properties. *J. Phys. Chem. B* **2011,** *115*, 9980-9989.
(16) Toutchkine, A.; Kraynov, V.; Hahn, K., Solvent-Sensitive Dyes to Report Protein Conformational Changes in Living Cells. *J. Am. Chem. Soc.* **2003,** *125*, 4132-4145.
(17) Sunahara, H.; Urano, Y.; Kojima, H.; Nagano, T., Design and Synthesis of a Library of BODIPY-Based Environmental Polarity Sensors Utilizing Photoinduced Electron-Transfer-Controlled Fluorescence ON/OFF Switching. *J. Am. Chem. Soc.* **2007,** *129*, 5597-5604.
(18) Duan, X.; Li, P.; Li, P.; Xie, T.; Yu, F.; Tang, B., The synthesis of polarity-sensitive fluorescent dyes based on the BODIPY chromophore. *Dyes Pigments* **2011,** *89*, 217-222.
(19) Klymchenko, A. S., Solvatochromic and Fluorogenic Dyes as Environment-Sensitive Probes: Design and Biological Applications. *Acc. Chem. Res.* **2017,** *50*, 366-375.
(20) Matsubara, R.; Yabuta, T.; Md Idros, U.; Hayashi, M.; Ema, F.; Kobori, Y.; Sakata, K., UVA- and Visible-Light-Mediated Generation of Carbon Radicals from Organochlorides Using Nonmetal Photocatalyst. *J. Org. Chem.* **2018,** *83*, 9381-9390.
(21) Greenspan, P.; Mayer, E. P.; Fowler, S. D., Nile red: a selective fluorescent stain for intracellular lipid droplets. *J. Cell Biol.* **1985,** *100*, 965-973.
(22) Smirnova, E.; Goldberg, E. B.; Makarova, K. S.; Lin, L.; Brown, W. J.; Jackson, C. L., ATGL has a key role in lipid droplet/adiposome degradation in mammalian cells. *EMBO reports* **2006,** *7*, 106-113.
(23) Fam, T. K.; Klymchenko, A. S.; Collot, M., Recent Advances in Fluorescent Probes for Lipid Droplets. *Materials (Basel, Switzerland)* **2018,** *11*, 1768.
(24) Hongji, J.; Jian, S.; Jinlong, Z., A Review on Synthesis of Carbazole-based Chromophores as Organic Light-emitting Materials. *Curr. Org. Chem.* **2012,** *16*, 2014-2025.
(25) Xu, S.; Liu, T.; Mu, Y.; Wang, Y.-F.; Chi, Z.; Lo, C.-C.; Liu, S.; Zhang, Y.; Lien, A.; Xu, J., An Organic Molecule with

Asymmetric Structure Exhibiting Aggregation-Induced Emission, Delayed Fluorescence, and Mechanoluminescence. *Angew. Chem. Int. Ed.* **2015,** *54*, 874-878.
(26) Chen, S.; Qin, Z.; Liu, T.; Wu, X.; Li, Y.; Liu, H.; Song, Y.; Li, Y., Aggregation-induced emission on benzothiadiazole dyads with large third-order optical nonlinearity. *Phys. Chem. Chem. Phys.* **2013,** *15*, 12660-12666.
(27) Chen, S.; Chen, N.; Yan, Y. L.; Liu, T.; Yu, Y.; Li, Y.; Liu, H.; Zhao, Y. S.; Li, Y., Controlling growth of molecular crystal aggregates for efficient optical waveguides. *Chem. Commun.* **2012,** *48*, 9011-9013.
(28) Bixon, M.; Jortner, J.; Cortes, J.; Heitele, H.; Michel-Beyerle, M. E., Energy Gap Law for Nonradiative and Radiative Charge Transfer in Isolated and in Solvated Supermolecules. *J. Phys. Chem.* **1994,** *98*, 7289-7299.
(29) Grabowski, Z. R.; Rotkiewicz, K.; Rettig, W., Structural changes accompanying intramolecular electron transfer: focus on twisted intramolecular charge-transfer states and structures. *Chem. Rev.* **2003,** *103*, 3899-4032.
(30) Sasaki, S.; Drummen, G. P. C.; Konishi, G.-i., Recent advances in twisted intramolecular charge transfer (TICT) fluorescence and related phenomena in materials chemistry. *J. Mater. Chem. C* **2016,** *4*, 2731-2743.
(31) Rettig, W., Charge Separation in Excited States of Decoupled Systems—TICT Compounds and Implications Regarding the Development of New Laser Dyes and the Primary Process of Vision and Photosynthesis. *Angewandte Chemie International Edition in English* **1986,** *25*, 971-988.
(32) Rotkiewicz, K.; Grellmann, K. H.; Grabowski, Z. R., Reinterpretation of the anomalous fluorescense of p-n,n-dimethylamino-benzonitrile. *Chem. Phys. Lett.* **1973,** *19*, 315-318.
(33) Reinterpretation of the anomalous fluorescence of p-N,N-dimethylamine-benzonitrile: Chem. Phys. Letters 19 (1973) 315. *Chem. Phys. Lett.* **1973,** *21*, 212 (erratum).
(34) Jones, G.; Jackson, W. R.; Halpern, A. M., Medium effects on fluorescence quantum yields and lifetimes for coumarin laser dyes. *Chem. Phys. Lett.* **1980,** *72*, 391-395.
(35) Hamada, H.; Tsuji, H.; Nakamura, E., Aggregation-responsive ON–OFF–ON fluorescence-switching behaviour of twisted tetrakis(benzo[b]furyl)ethene made by hafnium-mediated McMurry coupling. *Mater. Chem. Front.* **2018,** *2*, 296-299.
(36) Hu, R.; Lager, E.; Aguilar-Aguilar, A.; Liu, J.; Lam, J. W. Y.; Sung, H. H. Y.; Williams, I. D.; Zhong, Y.; Wong, K. S.; Peña-Cabrera, E.; Tang, B. Z., Twisted Intramolecular Charge Transfer and Aggregation-Induced Emission of BODIPY Derivatives. *J. Phys. Chem. C* **2009,** *113*, 15845-15853.
(37) Murphy, D. J., The biogenesis and functions of lipid bodies in animals, plants and microorganisms. *Prog. Lipid Res.* **2001,** *40*, 325-438.
(38) Fujimoto, T.; Ohsaki, Y.; Cheng, J.; Suzuki, M.; Shinohara, Y., Lipid droplets: a classic organelle with new outfits. *Histochem. Cell Biol.* **2008,** *130*, 263-79.
(39) Huang, L.; Ma, P.; Deng, G.; Zhang, K.; Ou, T.; Lin, Y.; Wong, M. S., Novel electron-deficient quinoxalinedithienothiophene- and phenazinedithienothiophene-based photosensitizers: The effect of conjugation expansion on DSSC performance. *Dyes Pigments* **2018,** *159*, 107-114.
(40) Mann, G.; Hartwig, J. F.; Driver, M. S.; Fernández-Rivas, C., Palladium-Catalyzed C−N(sp^2) Bond Formation: N-Arylation of Aromatic and Unsaturated Nitrogen and the Reductive Elimination Chemistry of Palladium Azolyl and Methyleneamido Complexes. *J. Am. Chem. Soc.* **1998,** *120*, 827-828.

AUTHOR INFORMATION

Corresponding Author

* matsubara.ryosuke@people.kobe-u.ac.jp

ACKNOWLEDGMENT

This work was carried out by the joint research program of Molecular Photoscience Research Center, Kobe University (H29001, H30021). We thank Profs. Atsunori Mori and Kentaro Okano for their help on mass analysis, and Profs. Yasuhiro Kobori, Manabu Sakurai and Naoki Yamamoto for their helpful discussion. Prof. Atsuo Tamura and Haruka Sakurai are acknowledged for the help on DLS analysis, and Profs. Satoshi Minakata and Yohei Takeda for the help on fluorescence measurements. Financial supports from JSPS KAKENHI Grant Number JP16K18844, Shorai Foundation for Science and Technology, and Research Foundation for Opto-Science and Technology are greatly appreciated.

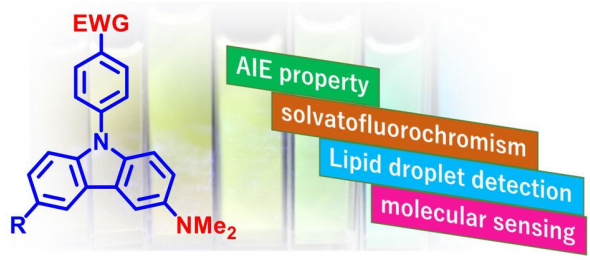
EWG
N
R
NMe2
AIE property
solvatofluorochromism
Lipid droplet detection
molecular sensing